Three-dimensional imaging of human hippocampal tissue using synchrotron radiation- and grating-based micro computed tomography

Simone E. Hieber*[a], Anna Khimchenko[a], Christopher Kelly[b], Luigi Mariani[b], Peter Thalmann[a], Georg Schulz[a], Rüdiger Schmitz[a], Imke Greving[c], Marco Dominietto[a], and Bert Müller[a]
[a]Biomaterials Science Center, c/o University Hospital Basel, 4031 Basel, Switzerland;
[b]Neurosurgery, University Hospital Basel, 4031 Basel, Switzerland;
[c]Institute of Materials Research (HZG), Max Plank Str. 1, 21502 Geesthacht, Germany

ABSTRACT

Hippocampal sclerosis is a common cause of epilepsy, whereby a neuronal cell loss of more than 50 % cells is characteristic. If medication fails, the best possible treatment is the extraction of the diseased organ. To analyze the microanatomy of the diseased tissue, we scanned a human hippocampus extracted from an epilepsy patient. After the identification of degenerated tissue using magnetic resonance imaging, the specimen was reduced in size to fit into a cylindrical container with a diameter of 6 mm. Using synchrotron radiation and grating interferometry we acquired micro computed tomography datasets of the specimen. The present study was one of the first successful phase tomography measurements at the imaging beamline P05 (operated by HZG at the PETRA III storage ring, DESY, Hamburg, Germany). Ring and streak artifacts were reduced by enhanced flat-field corrections, combined wavelet-Fourier filters and bilateral filtering. We improved the flat-field correction by the consideration of the correlation between the projections and the flat-field images. In the present study, the correlation that was based on mean squared differences and evaluated on manually determined reference regions leads to the best artifact reduction. A preliminary segmentation of the abnormal tissue reveals that a clinically relevant study requires the development of even more sophisticated artifact reduction tools or a phase contrast measurement of higher quality.

Keywords: Phase contrast, grating interferometry, hippocampus, sclerosis, human brain, degenerated tissue, flat field correction

1. INTRODUCTION

The visualization of the human brain's microanatomy belongs to the great challenges in medical imaging. Although magnetic resonance imaging provides deep insights, the spatial resolution is insufficient to study the structure on the level of individual cells. The current knowledge on the brain's microanatomy relies on two-dimensional optical and electron microscopy techniques, which generally require demanding preparation procedures including sectioning and staining [1]. An alternative is hard X-ray grating interferometry. X-ray phase contrast microtomography provides the real part of the refractive index decrement of an object in three dimensions [2, 3]. The high sensitivity of grating-based phase contrast allows identifying tissue types in brain tissue of the human cerebellum [4]. A registration of the phase contrast micro computed tomograms of the cerebellum and the histological slices reveals the local strains due to the preparation procedure [5]. In addition to the superior contrast this experimental approach provides micrometer resolution to visualize larger biological cells without staining. The phase contrast measurements can also be performed using an asymmetric rotation axis to acquire data of specimens up to twice as large as the beam size [6, 7]. Here, the aim is to analyze the morphology and the internal structure of a hippocampal sclerosis extracted from a patient suffering from temporal lobe epilepsy. Hippocampal (mesiotemporal) sclerosis is the most common underlying cause of mesial temporal lobe epilepsy (81 %) [8]. Histology shows a characteristic neuronal loss of more than 50 % in the hippocampus. The cell loss leads to a reorganization of neuronal networks, which is believed to significantly contribute to the development of epilepsy [9]. A form of synaptic reorganization known as mossy fiber sprouting may cause recurrent excitation leading to a '*short circuit*' and thus to a seizure [10]. Prolonged status epilepticus results in considerable cell loss in hippocampal areas CA1, CA3, the hilus and middle layers of the entorhinal cortex, while cell loss itself is related to reorganization of neuro-

*simone.hieber@unibas.ch; phone 41 61 265 9112; fax 41 61 265 9659; bmc.unibas.ch

Developments in X-Ray Tomography IX, edited by Stuart R. Stock, Proc. of SPIE Vol. 9212,
92120S · © 2014 SPIE · CCC code: 0277-786X/14/$18 · doi: 10.1117/12.2061582

Downloaded From: http://proceedings.spiedigitallibrary.org/ on 10/20/2014 Terms of Use: http://spiedl.org/terms

nal networks and this reorganization may be involved in epileptogenesis [11]. The pathogenesis of hippocampal sclerosis is not completely understood. The clinical course appears to be progressive. Initially with antiepileptic drugs controlled seizures remerge and become medically intractable in up to 60 to 90 % of patients [11]. In such cases temporal lobe resection or selective amygdalohippocampectomy is the best possible treatment. In Switzerland, only a few hospitals, including the Neurosurgery Department of the University Hospital of Basel, are permitted to perform surgery to remove the epileptogenic cortex in patients. A structural insight might help understand this pathology and help develop further strategies to improve the treatment and outcome of patients. The present study presents the results of the phase micro-tomography measurement at the imaging beamline P05 operated by the Helmholtz Zentrum Geesthacht at the PETRA III storage ring, DESY, Hamburg, Germany towards the morphological analysis of a hippocampal sclerosis of a human being.

2. METHODS

2.1 Specimen preparation

As the medication for the patient was insufficient to treat the symptoms of epilepsy, the best alternative treatment was the extraction of the diseased hippocampus. The surgery was performed at the Neurosurgery Department of the University Hospital in Basel. After the extraction hippocampus was fixed in 4 % formalin [12] and the location of the degenerated tissue was identified using magnetic resonance imaging (4.7 T magnet, cryogenic coil) at the Institute for Biomedical Engineering, ETH Zurich, Zurich, Switzerland [4]. The RARE T2 weighted images were resolved in a pixel size of 33 µm × 60 µm. The specimen including the degenerated tissue was reduced in size to fit into a cylindrical container with a diameter of 6 mm. The procedure was conducted according to the declaration of Helsinki and followed ethical guidelines of the University Hospital of Basel, Basel, Switzerland.

2.2 Data acquisition

The phase-contrast X-ray tomography data were acquired at the imaging beamline (IBL / P05) at the storage ring PETRA III operated by the Helmholtz Zentrum Geesthacht (HZG, HASYLAB/DESY, Hamburg, Germany) [13]. The imaging beamline has a micro- and a nano-tomography station [14]. The micro tomography station is in user operation since 2013 and the absorption contrast methods are established. A recently implemented differential phase-contrast (DPC) setup based on a single grating was used to obtain one of the first successful DPC measurements. An analyzer grating was not implemented because the period of the beam splitter grating corresponding to 22.4 µm could be resolved by the pixel arrary of the detector. The optimal photon energy for this experiment was found to be 15 keV and a 5× optical magnification was chosen, resulting in an effective pixel size of 2.4 µm. As a scintillator a 300 µm-thick $CdWO_4$ crystal was integrated and a CCD camera (Digital Imaging System, 3056 x 3056, 12 µm pixel size) was applied to record the radiographs. 180° scans were acquired with equiangular steps for 299 or 499 projections in a total of ten height steps. Five phase steps per period were taken at each angle. Additionally for every block of 100 images one block of 25 reference images had to be recorded in order to compensate for beam instabilities. During the measurement the field of view was limited, since a margin of 40 pixels on both sides of the specimen was needed in order to correct for beam drift. The reconstruction procedure of the presented phase contrast measurements including the creation of the sinograms were performed using a modified filter kernel (Hilbert transform) in combination with a standard back-projection algorithm [15]. The data was binned with a factor of four [16]. The processing was performed using Matlab 2014a (MathWorks, Natick, USA).

2.3 Artifact reduction

Artifacts caused by beam instabilities were removed in the established attenuation-based tomography by the correlation of projections and reference images prior to reconstruction [17]. Since this methodology has not been established for phase-contrast measurements at the beamline P05, we developed an approach to improve the quality of the phase contrast tomograms. The ring and streak artifacts were significantly reduced by an advanced flat-field correction and image filtering.

Downloaded From: http://proceedings.spiedigitallibrary.org/ on 10/20/2014 Terms of Use: http://spiedl.org/terms

Flat-field correction

The procedure corrects for the variation in the pixel sensitivity of the detector and/or distortions in beam path by the consideration a flat-field image *IF*. The corrected projection *IC* is evaluated using the following equation,

$$IC = \frac{(IR - ID)m}{IF - ID} \tag{1}$$

where *IR* is the raw projection, *ID* the dark images and *m* the mean of the flat-field image after dark-field correction. During a typical measurement of one height step phase 625 flat-field images were captured for 2500 projections. The gold standard in flat-field correction is the random selection of the reference image *IF* within a block. In the present study we considered several approaches to improve the flat-field correction. Due to the instability of the beam profile the random choice of the flat field was insufficient for this measurement. To find the best matching reference image we choose the following kinds of correlation evaluations between projection and reference image:

- mean squared difference,
- mean absolute difference,
- normalized cross-correlation,
- correlation coefficients.

We compared the effect for the evaluation on the complete projections. The correlation using mean squared differences was investigated with respect to the following reference areas:

- complete image,
- observation area of fixed size at both lateral margins (2 × 80 × 430 pixels),
- manually determined reference areas with largest possible sizes to prevent overlaps with the specimen.

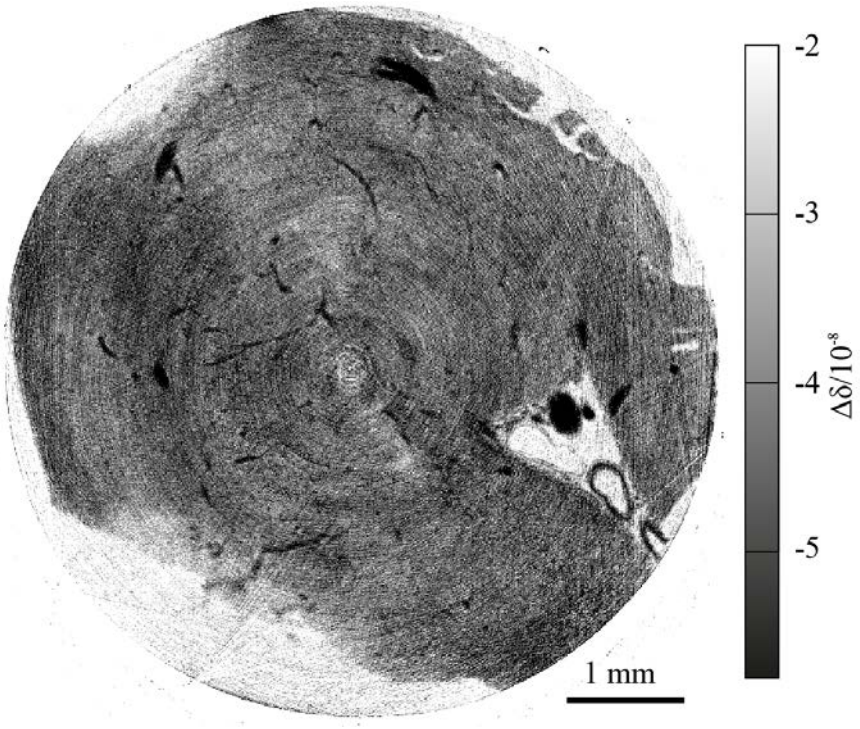

Figure 1. The slice reconstructed using standard flat-field correction shows the interior of a human hippocampus including blood vessels. The bright areas close to the center may represent abnormal tissue that can result from the sclerosis. Considerable ring and streak artifacts are present, which can be reduced by appropriate data processing.

Downloaded From: http://proceedings.spiedigitallibrary.org/ on 10/20/2014 Terms of Use: http://spiedl.org/terms

Image filtering

To further increase the quality of the data set a combined wavelet-Fourier filtering technique [18] was applied to the sinograms in the reconstruction procedure. It was already successfully used for microscopy images, computed tomography data, and grating interferometry projections. In the present study, particularly the high-frequency ring artifacts were reduced by this approach. The filter was used with the highest decomposition level $L = 3$; wavelet type db15 and damping factor $\sigma = 3.0$. Finally, an enhanced bilateral filter for DPC data was used for efficient de-noising [19], also experienced in recent measurements [20].

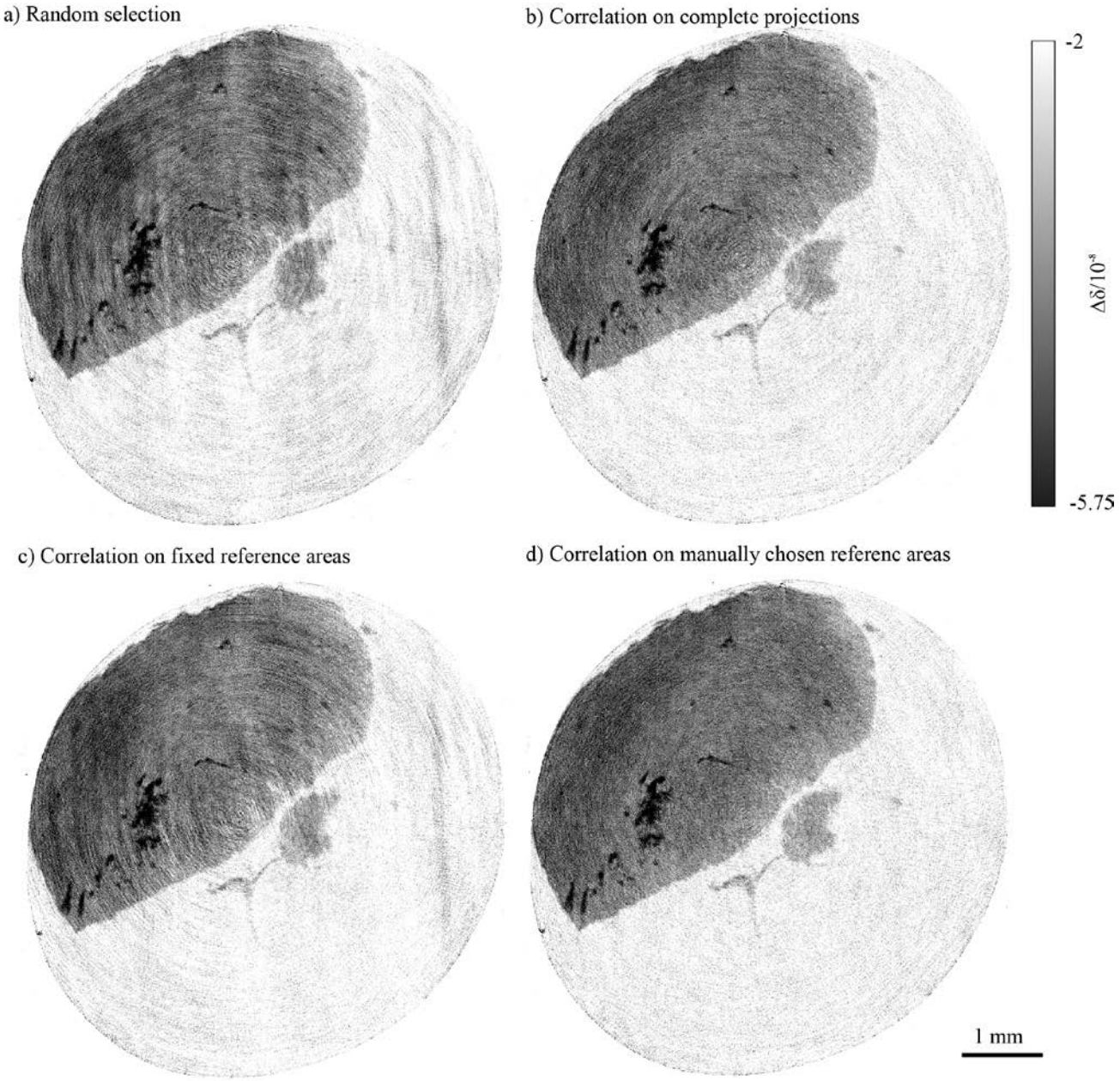

Figure 2. Effect of the flat-field correction: The standard approach includes a random selection of the flat-field images (top left). The artifacts are more efficiently reduced using a correlation-based selection considering complete projections (top right). Lateral reference areas of a fixed size resulted in minor reduction (bottom left), whereas manually selected areas led to the best result for the specific dataset (bottom right).

Downloaded From: http://proceedings.spiedigitallibrary.org/ on 10/20/2014 Terms of Use: http://spiedl.org/terms

3. RESULTS

The reconstructed data set revealed internal structures of the hippocampal tissue including vessels and indicated several types of tissue components. The very dark branches in Figure 1 and the few circular structures belong to the vessel tree. Their lumen is displayed in bright gray with $\Delta\delta = 2 \cdot 10^{-8}$ if filled with formalin instead of blood. The tissue exhibits light gray areas that can be identified as abnormal tissue, possibly a result of the sclerosis. The reconstructed slices feature considerable ring and streak artifacts. They might not only be attributed to defects in the detector pixel arrays and strongly X-ray-absorbing particles within the specimen, respectively, but they could also be caused by the instability of the monochromatic X-ray beam. The artifacts are predominately a result from the reconstruction of the standard flat-field corrected radiographs using a random selection of flat fields. The consideration of a correlation between the projection and the flat-field image improved the quality of the images as shown in Figure 2. In general, the correlations were not related to the corresponding blocks. When comparing the effect of the correlation approaches, the application of mean squared difference led to the best artifact reduction in the data analyzed. Particularly, the streak artifacts were suppressed by an appropriate choice of the correlation method. Figure 2 shows that the application of an appropriate correlation reduced the streak artifacts significantly, whereas the choice of the reference area for the correlation had a higher impact on the ring artifacts. After the manual selection of the largest possible areas without a specimen the flat-field correction resulted in slices of such high level quality that further processing could be omitted.

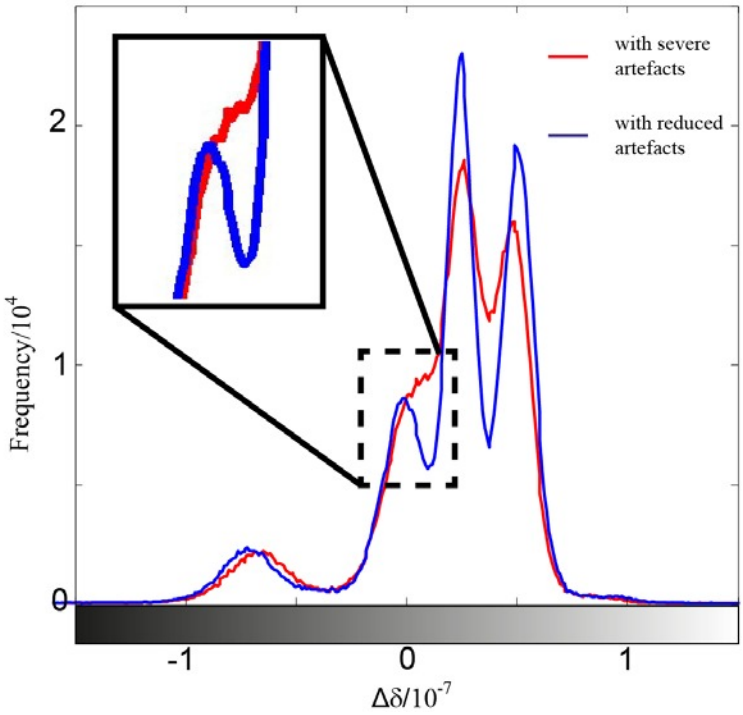

Figure 3. The improved choice of the flat-field correction revealed a peak in the histogram based on the selected slice showing the real part of the refractive index (blue). The peak was hidden in the histogram for the same slice featuring severe artifacts (red).

Downloaded From: http://proceedings.spiedigitallibrary.org/ on 10/20/2014 Terms of Use: http://spiedl.org/terms

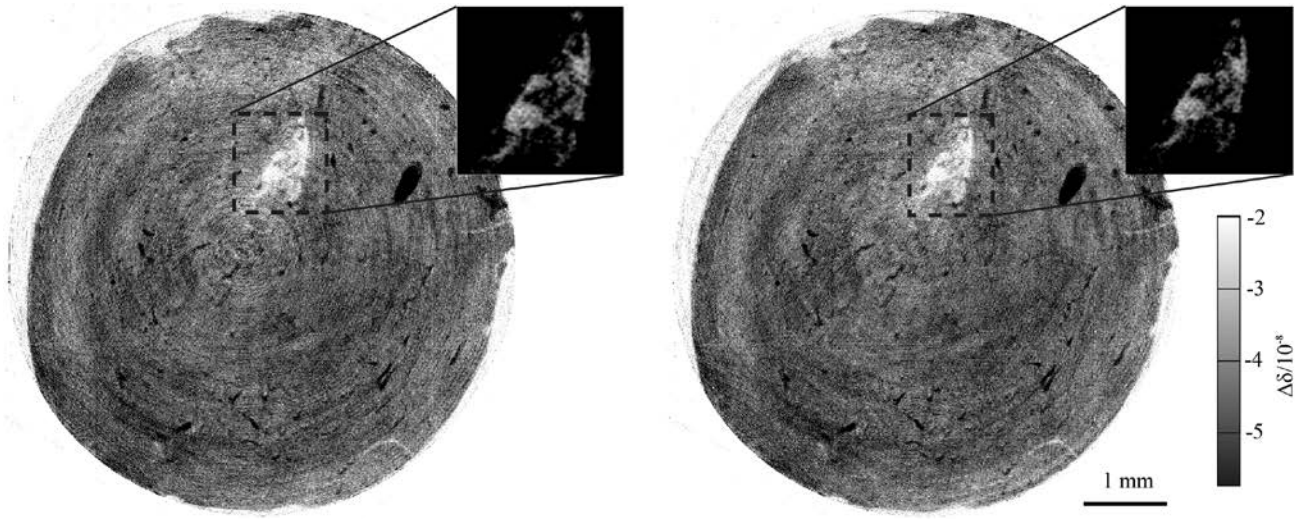

Figure 4. Slice reconstructed from original sinograms (left) and from wavelet Fourier filtered ones (right). The insets are de-noised using bilateral filtering.

The flat-field correction can have a significant impact on the histogram as shown in Figure 3. It shows that the artifact reduction can facilitate the recognition of a third peak in the histogram and thus improve the further analysis significantly. The combined wavelet Fourier filter was capable of handling ring artifacts of high frequency and revealing small-scale structures of the brain sample. Figure 4 compares a slice including abnormal tissue (bright area) reconstructed without (left) and with the wavelet-Fourier filtered sinogram (right). The inlets correspond to bilateral filtered images. Most of the ring artifacts, in particular the high-frequency ones, are well addressed by the filter. Low-frequency rings are still visible but do not affect severely the main structure such as the vessels and the abnormal tissue. After bilateral filtering the difference between the slices is hardly recognizable as shown in the insets. Thus, the de-noising algorithm is also capable of reducing ring artifacts.

4. DISCUSSION

The flat-field correction is essential for the artifact reduction in the DPC measurement of brain tissue specimen. The artifacts were mainly caused by the beam instabilities during the measurement, which are most likely caused by the liquid nitrogen-cooled monochromator. To reduce the resulting artifacts in the phase-contrast measurements we followed several approaches to improve the flat-field selection established in attenuation-based tomography. Comparing the correlations, mean squared difference lead to better results when considering the complete projection. The consideration of a fixed region within the margin reduced the artifacts as well, but the quality depended on the size of the region and might show a less optimized result compared to the use of the complete projections. Since the approach based on the complete projections showed a better reduction of artifacts in Figure 2, the size of the chosen region was probably insufficient for a suitable flat-field correction. When optimizing the size of the region, best results were found by manually chosen regions for the projections. The manual approach, however, is very time-consuming, because one height step required about eight hours working time of an expert. Therefore, an automatic determination would be desirable for example using edge detection. The wavelet-Fourier filtering procedure allowed the damping of high-frequency ring artifacts but broad ring-like structures remained that could still have an impact on the segmentation of the abnormal tissue. Bilateral filtering reduced the noise in the images efficiently, but the quantitative information of the refractive index is distorted because the histogram is transformed nonlinearly. Thus, de-noising is useful for further processing steps such as segmentation.

5. CONCLUSIONS

The present paper reports the first grating-based phase-contrast measurement at the recently established beamline P05 at the PETRA III storage ring, DESY, Hamburg, Germany. The reconstructed slices suffered from several artifacts mainly caused by the instability of the monochromized X-ray beam. Ring and streak artifacts could be significantly reduced by flat-field correction and wavelet filtering.

Downloaded From: http://proceedings.spiedigitallibrary.org/ on 10/20/2014 Terms of Use: http://spiedl.org/terms

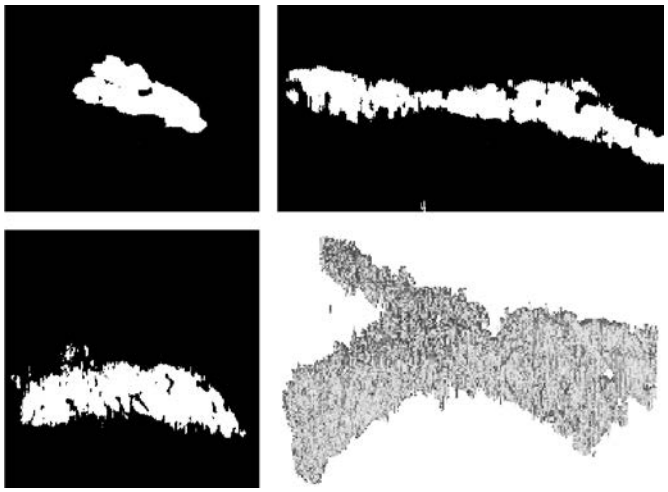

Figure 5. The three-dimensional segmentation of the abnormal tissue within one height step based on thresholding (Otsu's method) combined with a sliding window approach. The preliminary data are to be handled with care and give an impression on the three-dimensional structure of the diseased brain tissue from both the orthogonal virtual cuts and the three-dimensional representation. The images also support the planning of the histological sectioning, necessary to identify the healthy and diseased regions as well as the density of cells. The anatomical features allow the navigation within the specimen. Here, the vessels are the most prominent features, which can be even optically seen at the periphery of the cylindrically shaped specimen.

The choice of highly correlated the flat-field images reduced the artifacts significantly such that further filtering could be omitted. Bilateral filtering was an effective tool for de-noising for a later segmentation. The segmentation of the abnormal tissue in the data set with reduced artifacts indicates the complexity of its morphology (cp. Figure 5). A clinically relevant segmentation requires the development of even more sophisticated artifact reduction tools or a phase contrast measurement of higher quality as already performed at the beamline ID 19 (ESRF, Grenoble, France). Finally, it is planned to prepare the specimen for sectioning and immunohistochemical staining to identify the tissues in the specimen histologically. The three-dimensional dataset is expected to represent the morphological data of the brain sclerosis, which are important for the successful planning and successful patient treatment in neurosurgery.

ACKNOWLEDGMENTS

The authors gratefully acknowledge Julia Herzen, Alexander Hipp and Felix Beckmann for the technical implementation of the single grating phase contrast technique at P05 imaging beamline and Pavel Lytaev for his support at the beamline. We also thank Simon Pezold from the Medical Image Analysis Center, University of Basel, for his advice concerning the segmentation. The project was supported by beam time from the photon science initiative at DESY, Hamburg, Germany (proposal I-20130358).

REFERENCES

[1] Morel, A., [Stereotactic atlas of the human thalamus and basal ganglia] Informa Healthcare New York(2007).

[2] Atsushi, M., Shinya, K., Ichiro, K., Yoshitaka, H., Kengo, T., and Yoshio, S., "Demonstration of X-Ray Talbot Interferometry," Jpn. J. Appl. Phys. 42(7B), L866 (2003).

[3] Weitkamp, T., Diaz, A., David, C., Pfeiffer, F., Stampanoni, M., Cloetens, P., and Ziegler, E., "X-ray phase imaging with a grating interferometer," Opt. Express 13(16), 6296-6304 (2005).

Downloaded From: http://proceedings.spiedigitallibrary.org/ on 10/20/2014 Terms of Use: http://spiedl.org/terms

[4] Schulz, G., Weitkamp, T., Zanette, I., Pfeiffer, F., Beckmann, F., David, C., Rutishauser, S., Reznikova, E., and Muller, B., "High-resolution tomographic imaging of a human cerebellum: comparison of absorption and grating-based phase contrast," J. R. Soc. Interface 7(53), 1665-1676 (2010).

[5] Schulz, G., Morel, A., Imholz, M., Deyhle, H., Weitkamp, T., Zanette, I., Pfeiffer, F., David, C., Müller-Gerbl, M., and Müller, B., "Evaluating the microstructure of human brain tissues using synchrotron radiation-based micro computed tomography," Proc. SPIE 7804, 78040F (2010).

[6] Schulz, G., Weitkamp, T., Zanette, I., Pfeiffer, F., Müller-Gerbl, M., David, C., and Müller, B., "Asymmetric rotational axis reconstruction of grating-based X-ray phase contrast tomography of the human cerebellum," Proc. SPIE 8506, 850604 (2012).

[7] Müller, B., Bernhardt, R., Weitkamp, T., Beckmann, F., Bräuer, R., Schurigt, U., Schrott-Fischer, A., Glueckert, R., Ney, M., Beleites, T., Jolly, C., and Scharnweber, D., "Morphology of bony tissues and implants uncovered by high-resolution tomographic imaging " Int. J. Mater. Res. 98(7), 613-621 (2007).

[8] Williamson, P. D., French, J. A., Thadani, V. M., Kim, J. H., Novelly, R. A., Spencer, S. S., Spencer, D. D., and Mattson, R. H., "Characteristics of medial temporal lobe epilepsy: II. Interictal and ictal scalp electroencephalography, neuropsychological testing, neuroimaging, surgical results, and pathology," Ann. Neurol. 34(6), 781-7 (1993).

[9] Blumcke, I., Thom, M., and Wiestler, O. D., "Ammon's horn sclerosis: a maldevelopmental disorder associated with temporal lobe epilepsy," Brain Pathol. 12(2), 199-211 (2002).

[10] Nadler, J. V., "The Recurrent Mossy Fiber Pathway of the Epileptic Brain," Neurochem. Res. 28(11), 1649-1658 (2003).

[11] Heinemann, U., "Basic mechanisms of partial epilepsies," Curr. Opin. Neurol. 17(2), 155-9 (2004).

[12] Schulz, G., Crooijmans, H., Germann, M., Scheffler, K., Müller-Gerbl, M., and Müller, B., "Three-dimensional strain fields in human brain resulting from formalin fixation," J. Neurosci. Meth. 202, 17-27 (2011).

[13] Haibel, A., Beckmann, F., Dose, T., Herzen, J., Ogurreck, M., Müller, M., and Schreyer, A., "Latest developments in microtomography and nanotomography at PETRA III," Powder Diffraction 25, 161-164 (2010).

[14] Ogurreck, M., Wilde, F., Herzen, J., Beckmann, F., Nazmov, V., Mohr, J., Haibel, A., Müller, M., and Schreyer, A., "The nanotomography endstation at the PETRA III Imaging Beamline," J. Phys.: Conf. Ser. 425(18), 182002 (2013).

[15] Pfeiffer, F., Bunk, O., Kottler, C., and David, C., "Tomographic reconstruction of three-dimensional objects from hard X-ray differential phase contrast projection images," Nucl.Instrum. Methods Phys. Res. A 580(2), 925-928 (2007).

[16] Thurner, P., Beckmann, F., and Müller, B., "An optimization procedure for spatial and density resolution in hard X-ray micro-computed tomography " Nucl. Instrum. Methods Phys. Res. B 225(4), 599-603 (2004).

[17] Greving, I., Wilde, F., Ogurreck M., Herzen J., Hammel, J., Hipp, A., Friedrich, F., Lottermoser, L., Dose T., Burmester, H., Müller, M., and Beckmann, F., "In Current Issue," Proc. SPIE 9212, (2014).

[18] Münch, B., Trtik, P., Marone, F., and Stampanoni, M., "Stripe and ring artifact removal with combined wavelet-Fourier filtering," Opt. Express 17(10), 8567-8591 (2009).

[19] Koehler, T., and Roessl, E., "Simultaneous de-noising in phase contrast tomography," AIP Conf. Proc. 1466(1), 78-83 (2012).

[20] Herzen, J., Willner, M. S., Fingerle, A. A., Noël, P. B., Köhler, T., Drecoll, E., Rummeny, E. J., and Pfeiffer, F., "Imaging Liver Lesions Using Grating-Based Phase-Contrast Computed Tomography with Bi-Lateral Filter Post-Processing," PLoS ONE 9(1), e83369 (2014).

Downloaded From: http://proceedings.spiedigitallibrary.org/ on 10/20/2014 Terms of Use: http://spiedl.org/terms